Ab initio simulations in liquid caesium at high pressure and temperature

S. Falconi and G. J. Ackland
School of Physics and Centre for Science at Extreme Conditions, The University of Edinburgh, Mayfield Road, Edinburgh EH9 3JZ, United Kingdom

(Received 1 February 2006; revised manuscript received 22 March 2006; published 22 May 2006)

The structure of liquid caesium undergoes a sharp change at around 4 GPa from a simple liquid to a low-coordination complex structure. This mirrors a similar change in the crystal structure at this pressure. Here, we show that both changes are accurately described in good agreement with experiment by density functional theory calculations, which shed light on the nature of the liquid structure and its electronic origins. Analysis of the wave function character shows *s-d* hybridization, but not *s-d* transfer, in both solid and liquid at the pressure of the complex Cs-III phase. This implies that a nearly free electron picture is more appropriate than one based on the atomic orbitals. The similarity of *s-d* hybridization in crystal and liquid phases indicates that hybridization is a general consequence of densification, rather than being induced by a particular crystal structure. The free-electron picture predicts that stable structures will have diffraction peaks associated with the Fermi vector, and this is borne out by comparison with experiment.

DOI: 10.1103/PhysRevB.73.184204 PACS number(s): 64.70.Ja, 62.50.+p, 64.60.My, 64.70.Fx

I. INTRODUCTION

In a recent paper the structural evolution with pressure of liquid Cs has been studied.[1] Liquid Cs exhibits a pressure induced structural change evident because of the appearance of an asymmetry in the first peak of the x-ray diffraction structure factor, $S(q)$, at high pressure and mainly explained as a densification of the liquid.[1] This densification phenomenon is also coupled with a counterintuitive reduction in the coordination number: from 12 near neighbors at ambient condition to 7–8 near neighbors at 9.8 GPa.[1]

The liquid structure analysis which revealed this entailed comparing the $S(q)$ profile with a hard sphere model[2,3] (HS): the HS model fits well at low pressure, but starts to fail at pressures above 3.6 GPa when a shoulder in the $S(q)$ profile starts to appear. This allows the liquid to be classified as a simple liquid up to 3.6 GPa. Beyond this, it is a "nonsimple liquid"—a structure for which no simple model exists. A similar study of the $S(q)$ profile has been also performed in liquid Rb (Ref. 4) and in other liquid systems that exhibit a change in the shape of the $S(q)$ profile.[5]

In the case of caesium a similar densification and change in the coordination number has been observed experimentally in the solid phase in the same pressure range.[6,7] Several numerical studies have been also performed even if none of them have shown the appropriate details[8] and/or the right phase transition sequence[9–11] until recently.[12–15]

The reported isostructural phase transition in caesium[9] occurs in the same pressure range as the liquid structure anomaly. It has attracted a great deal of theoretical interest for over 40 years. In particular, since the shape of the Brillouin zone is unchanged in an isostructural transition, effects such as stabilization by free electron Fermi surface effects could safely be discarded. The picture of a transition based on electron localization accompanying the *s-d* transfer became established and electron localization models at various levels of complexity which show isostructural transition have been constructed. The change is accompanied by a sharp decrease in conductivity, which has been attributed to electron localization,[17] and the increased *d* character can be inferred from Mossbauer spectroscopy.[18]

Electronic structure calculation based on the density functional theory (DFT) with local or semilocal exchange-correlation functionals proved unable to describe the isostructural transition.[3,8,10,11] This failure provided further evidence for the localization argument the *d*-localized system would have strong electron correlation effects for which such approaches are known to fail—as in *f*-electron metals such as cerium. Alternately, the isostructural transition has been explained as a thermal effect[10] due to soft phonons. Although recent calculations and experiment report a fcc phonon instability and other anomalies such as negative thermal expansion,[8,19–21] the details of these calculations do not suggest dynamically stabilized fcc.

This theorizing has recently been made redundant because the second high pressure phase transition between the phases conventionally denoted Cs II and Cs III at around 4.2 GPa is not isostructural. Instead, it is between fcc and a complex orthorhombic structure with 84 atoms in a C-centered unit cell.[6] The correct phase transition sequence at ambient temperature is Cs I(bcc) $\rightarrow$ Cs II(fcc) $\rightarrow$ Cs(III) (complex orthorhombic) $\rightarrow$ Cs IV (tetragonal) between a pressure range of 0 and 10 GPa.[15] Thus, the experimental observation which seemed explicable only by *d* localization is gone. As we shall see, this sequence can be well described by standard 0 K DFT methods plus phonon entropy.

Electronic structure models for Cs fall into two camps. Early simulation work[10] considered atom-centered orbitals and related the compression to the *s* to *d* electron transfer up to 4.5 GPa. Above that pressure ($V/V_0 \leqslant 0.43$) the 5*p* orbital also contributed to the compression process.[10] A recent canonical two-band model[12] showed qualitatively that this can cause an isostructural discontinuous volume change.

An alternate picture[22] starts with a free electron gas, and considers ionic perturbations about it: here the ions arrange themselves so as to lower the energy of the nearly free electron gas, for example by opening pseudogaps at the Fermi surface. Recent work shows qualitatively that this[13,23] leads

to complex crystal structures such as Cs III. These two pictures ultimately are just focusing on different basis sets: the agreement of total energy calculations based on plane waves or atomic orbital basis sets shows that when fully converged with respect to basis set they are ultimately equivalent.

In this paper, we show that DFT calculations do in fact provide a satisfactory description of the experimental phases of Cs—both liquid and solid. There is no need to treat electron correlation in detail. We reproduce recent work on the crystal phases[14] and present a study of a complex liquid. The simulations allow us to extract details of the liquid's ionic to compare with the experimental data and electronic structure which is very difficult to determine experimentally under high pressure and temperature.

II. METHODS

The calculations were carried out using the pseudopotential plane-wave method implemented via the VASP code.[24] An ultrasoft pseudopotential was used describing a Cs^{7+} ion (i.e., the $5p$ electrons are treated as valence: these states lie around 8 eV below the $6s$ bands, and do not hybridize, but their dispersion is altered at high pressure). The plane wave cutoff was set to 127 eV with a 246 eV cutoff for the augmentation charge. These values converge the fcc-bcc energy difference to within 0.3 meV/atom at 8.4 GPa, compared with a 1000 eV cutoff. The exchange correlation effects were described in the generalized gradient approximation (GGA) using the so-called PW-GGA-II potential[25] which generally gives a better description of high pressure phases than the local density approximation (LDA) which tends to give systematically too small a pressure.[26] Determination of electron localization and angular character was done by projection onto localized orbitals within a radius $(3\pi V/4)^{1/3}$ around each atom.

Crystal structure relaxation was done at fixed pressure using the Parrinello-Rahman method[27] which allows minimization of the energy with respect to all ionic at lattice degrees of freedom within the experimentally determined space group. The liquid calculations were done at constant volume and fixed temperature, using the Nosé-Hoover thermostat.[28] The structure at various pressures and temperatures was coarsely mapped using a 64 atom supercell interesting regions were probed using a 264 atom cell with totally different starting conditions.[29]

Liquid structure was analyzed through the radial distribution function, $g(r)$ and the angular distribution function $\Theta(\theta)$ between triplets of atoms in the near-neighbor peak of the $g(r)$.

III. RESULTS

A. Crystal structure stability

Properties of crystal phases I–IV have been calculated as described above. The method has been shown to give good agreement with experiment for energy differences of a wide range of simple materials under pressure. Caesium provides the method with a difficult test because the enthalpy differences between the dissimilar structures are extremely small at all pressures. This, combined with the high compressibility means that even small errors in the total energy, or contributions from phonons at finite temperature, are magnified to large errors in the transition pressures.

We have calculated energies as a function of volume for Cs in each of its phases I–IV assuming the most recently reported crystal structures. Unlike cases such as Se,[30] where the crystal structures are very similar to one another, the very different atomic arrangements in Cs make the expected errors in the energy differences several milli-electron-volts (meV).

Our calculations are converged to within less than 0.5 meV with respect to energy cutoff: we tested up to 300 eV compared with the VASP "high-accurate" default of 132 eV. Similar accuracy with k-point sampling up to 27^3 for phases I, II, and IV, and up to 5^3 for the 42-atom cell of phase III. Comparing energy differences between the GGA and the local density approximation suggests an error of order 1 meV from choice of exchange correlation function.

Considering enthalpy at 0 K, our calculations suggest that Cs III is unstable with respect to Cs II or Cs IV at all pressures by at least 2 meV, this is within the k point and energy cutoff convergence error, but may be outwith the pseudopotential transferability error. It is in agreement with full potential calculations.[14] Zero-point phonon contributions to the enthalpy are significantly larger than this, and from the thermodynamic measurements[17] the entropic contribution to the free energy difference is about 4 meV per atom in favor of Cs III at room temperature. This is consistent with the phase diagram which shows the region of Cs III stability increasing with temperature, and with experiments suggesting that Cs III may exist only at temperatures above 200 K.[31]

Thus, once the temperature is properly accounted for our calculations and those of Ref. 14 indicate a near-degeneracy of the observed crystal structures at around 4.2 GPa. A detailed description of the orbital character of the electronic structure of Cs III is presented in Ref. 14 based on full potential calculations, localized basis sets, and LDA. We have used psuedopotentials, plane wave basis sets and GGA. The results of the two calculations are extremely similar: Cs III exhibits a dip in the density of states at the Fermi surface due to the interactions with the Brillouin zone boundary and strong d character to the orbitals. Given the similarity, we do not repeat the detailed discussion here, except to note that within DFT the analysis of high-pressure Cs appears to be independent of implementation details, and in agreement with the experiment.

B. Liquid structure

For liquid simulations, we first check the agreement between the experimental $S(q)$ and the calculated $g(r)$, for the structural arrangement of the atoms and a range of fixed volumes. If the data were perfect and complete, the information in these would be identical since $S(q)$ is the Fourier transform of $g(r)$ as it is there are some minor errors associated with the truncation of the data. Once we are confident that the structure is correct, we relate the structural changes to the electronic properties. To enable direct comparison with

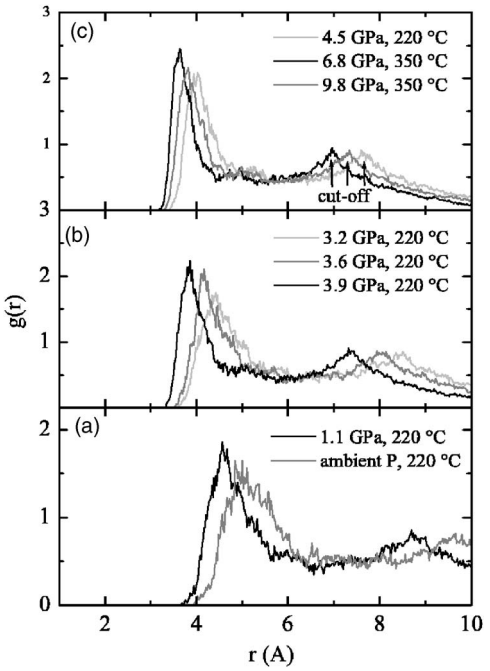

FIG. 1. $g(r)$ of liquid Cs obtained with a cluster of 64 atoms. Panel (a): $g(r)$ from ambient to 1.1 GPa; panel (b) $g(r)$ from 3.2 up to 3.9 GPa; panel (c): $g(r)$ from 4.5 up to 9.8 GPa. The first peak of $g(r)$ shows the near neighbor distance, while the integral under the peak gives the coordination number. The vertical arrows in panel (c) show the cutoff beyond which $g(r)$ is underestimated due to finite size of the super cell.

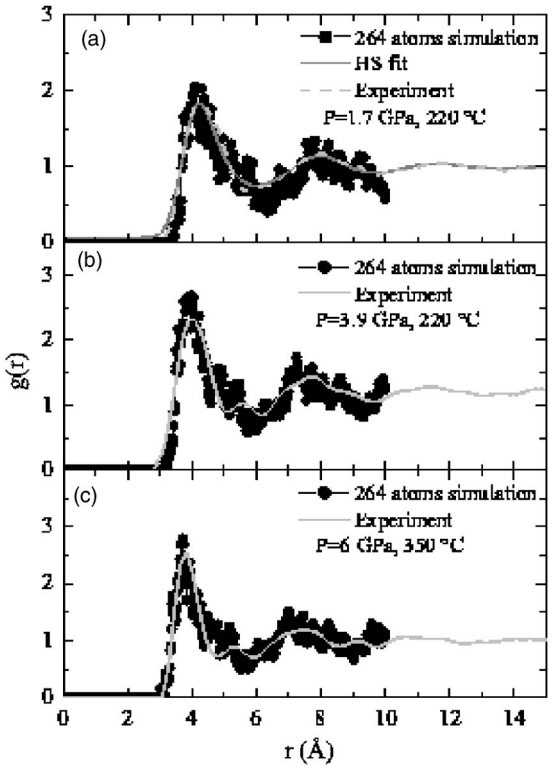

FIG. 2. $g(r)$ of liquid Cs obtained with a cluster of 264 atoms compared with experiment. The experimental $g(r)$ comes from Fourier transforming $S(q)$; there are extra small oscillations which are artifacts of this procedure.

experiment,[1] we simulate at 220 and at 350 °C between ambient pressure and 10 GPa.

The calculated $g(r)$ shows a gradual pressure-induced structural change (see Fig. 1) in agreement with the experiment. At ambient pressure and 220 °C, $g(r)$ shows a broad first peak at 5.06 Å [Fig. 1 panel (a)], as the pressure is increased the first peak of $g(r)$ shifts towards lower values as shown in the three panels of Fig. 1, reaching 3.6 Å at the highest pressures reached. At the structural transition, the peak develops a pronounced shoulder and a secondary peak seems to appear at about 7.5 Å. For our smaller simulation size, this is close to half the size of the simulation box, and so the peak is distorted by finite size effects. However, in the larger scale (264 atoms) simulations the peak is clearly observable, and the agreement with experiment is excellent (see Fig. 2).

Figure 3 shows the distance between near neighbors, d, obtained as the position of the first peak of the simulated $g(r)$ compared with the experimental values. The peak position of the $g(r)$ as a function of the pressure is in agreement with the experimental data at both temperatures investigated. Under compression the distance between near neighbors is enormously reduced, and, as experimentally observed, it is coupled with a big reduction in the coordination number from 12 near neighbors to 7–8 near neighbors at pressures which correspond to the transition from Cs II at 3.6 GPa to Cs IV at 4.5 GPa.[1]

Further structural analysis is provided by the study of the angular distribution of each atom within the distance of the neighbors closer than the first minimum of the $g(r)$. Although the strong change in the coordination number, C_{NN}, might suggest a preferential angular distribution around each atom, there is no strong evidence of it. In the Fig. 4 is shown the angular distributions $\Theta(\theta)$ corresponding to the $g(r)$ shown in Fig. 1. The strong peak characteristic of close-packing at 60 deg is visible at low pressures, but at high pressures distinct angular character is absent. This suggests

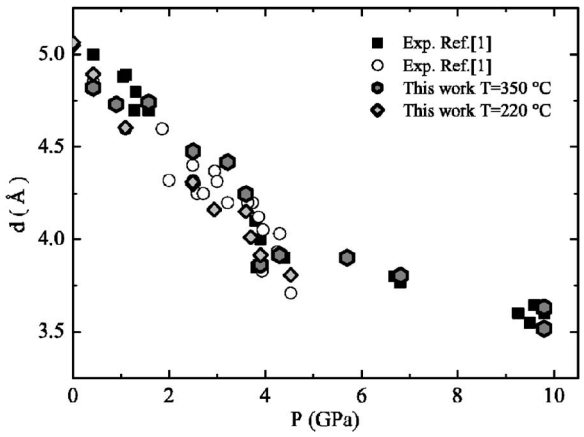

FIG. 3. Distance between near neighbors d as a function of pressure. The open circles and filled squares are the experimental data at 220 and 350 °C, respectively; the filled diamond and the filled hexagons are the simulated distances between near neighbors. Note the distinct change in slope between 4 and 5 GPa

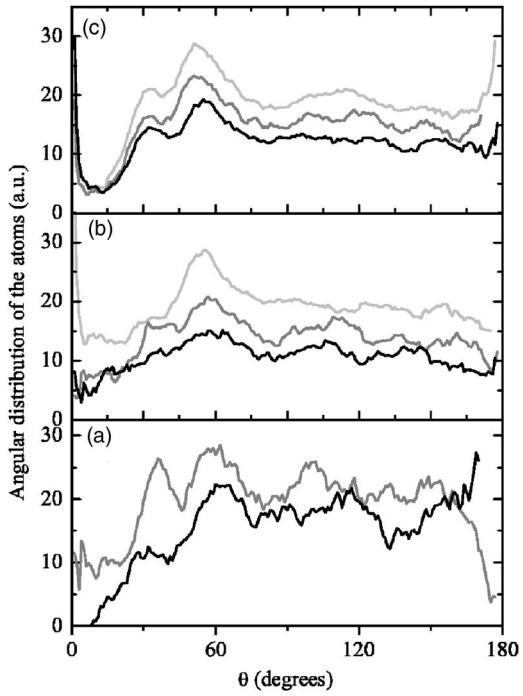

FIG. 4. Angular distribution between the atoms lying below the first minimum of the $g(r)$. Panel (a): distribution from ambient to 1.1 GPa; panel (b): distribution from 3.2 up to 3.9 GPa; panel (c): distribution from 4.5 up to 9.8 GPa. This figure uses a large range to define near neighbor—those with lengths below the lowest point between the first two peaks in the $g(r)$. Using a narrower distribution of neighbors has the effect of removing the low-angle peaks, but does not produce any further structure at high angle.

that the structure is not dominated by electrons with any particular pure angular character.

C. Comparison with experiment

The impressive structural agreement between calculations and experiment shown in Fig. 2 and Fig. 3 shows that the discontinuity in the near neighbor separations with pressure is well reproduced by the calculations. To better understand the coordination number behavior and the angular distributions in Fig. 4 we also consider the equation of state (EOS) in Fig. 5. This shows that liquid Cs is highly compressible up to 4.5 GPa, and above ~3 GPa, it is denser than the "close packed" solid. Like the solid, it has a sharp densification (very high compressibility) in the pressure region between the Cs II phase and the Cs III phase. Subsequently, it is less compressible for all pressures above 4.5 GPa and less dense than the solid. This further emphasizes that the low pressure structures are best thought of as ions avoiding one another in a free electron gas, rather than packing closely together. Our calculated liquid and solid EOS are in agreement with the x-ray experimental work[1,6,16] and the shock wave EOS.[10] In particular, both the experiment and *ab-initio* simulations show that in the pressure region below 4.2 GPa, the liquid is much more compressible than the solid, becoming denser than the solid above 3 GPa. The volume collapse at the Cs II–III–IV phase transitions around 4.3 GPa makes the solid

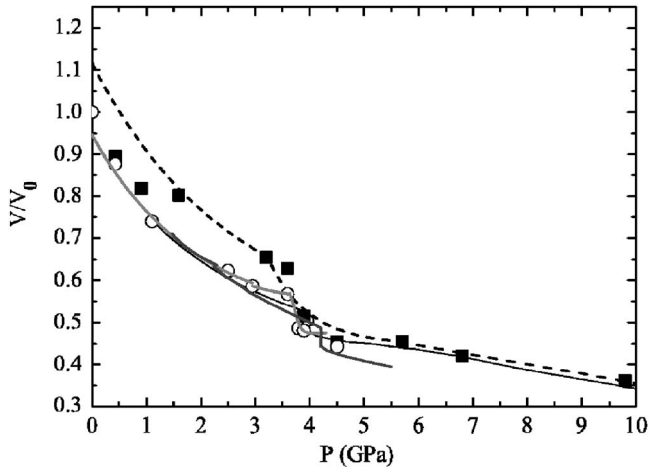

FIG. 5. V/V_0 vs pressure. The thick and thin solid black lines are the shock-wave experiment and previous theoretical estimation of the EOS in solid Cs (see Ref. 10). The black dashed and light gray lines are the experimental values at 220 and 350 °C, respectively (see Ref. 1). Open circles and filled squares are molecular dynamics calculations at 220 and 350 °C from the present work.

denser again.[1,7,17] It is thus clear that the calculation of high-pressure caesium using pseudopotential-DFT gives a good description of the structure, without requiring *d* localization for the volume collapse or temperature effects to stabilize the crystal structures. We can, therefore, examine our DFT electronic structure in detail, confident that it is a reasonable description of the real material.

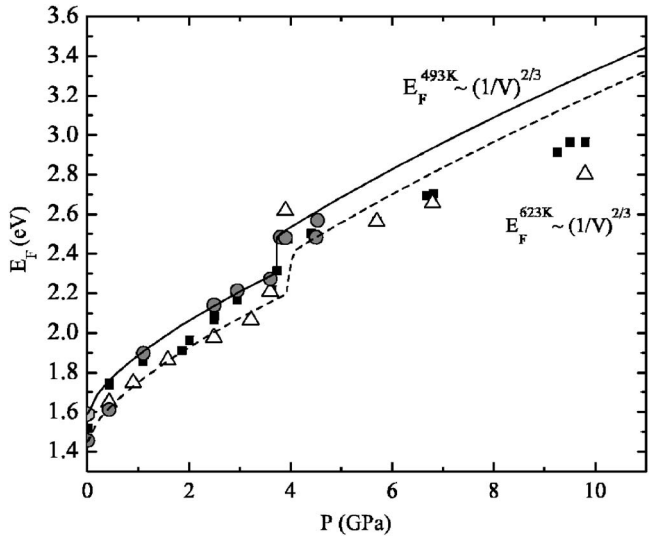

FIG. 6. Fermi energy as a function of pressure. The filled circles are the liquid-Cs calculations at 220 °C, the open triangles are the data at 350 °C and the full squares are the Fermi energy estimated from the experimental data (see Ref. 1). The solid line and the dashed lines are the Fermi levels in the case of a noninteracting Fermi gas ($E_F \propto V^{-2/3}$) at the experimental density with one electron per atom. For comparison, in each case we take the P=0 value for the Fermi level from literature data (Ref. 32).

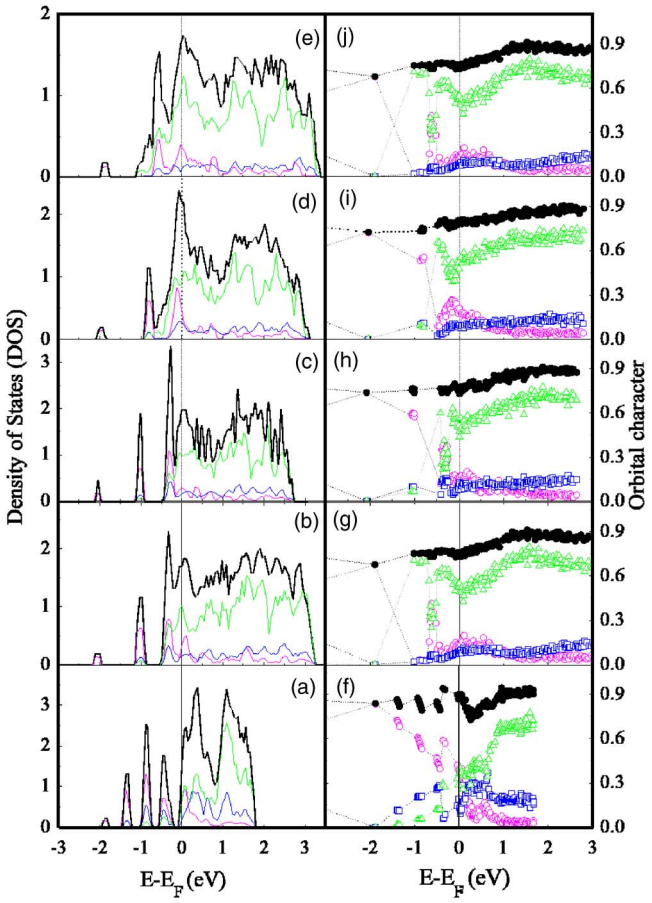

FIG. 7. (Color online) DOS and orbital character of electronic states for liquid Cs close to the melting curve at various pressures. Left hand panels show the density of states with each state broadened by 0.01 eV. Right hand panels show, for each state, the projected fraction of *s*, *p*, and *d* like states. Black lines represent the total DOS or sum of the *spd*-projected orbital character, with colors for the projection onto angular states: magenta (open circles) *s* state; blue (open squares) *p* state; green (open up-triangles) *d* state. The panels (a) and (f) are the data at ambient conditions, (b) and (g) are at 3.8 GPa and 220 °C, (c) and (h) are at 4.2 GPa and 220 °C, (d) and (i) are the data at 6.8 GPa and 350 °C and, finally, (e) and (l) are the data at 9.8 GPa and 350 °C. The vertical line indicates the Fermi level, and as usual with DFT calculation the character of unoccupied states above the Fermi energy should be treated with caution. The 5*p* states lie some 10 eV below the other valence states, and are not shown. The projected DOS are obtained as a weighted average of the partial DOS calculated at every single atomic site (64 atoms). The low energy "peaks" in (a)–(e) are an artifact of the *k*-point sampling (see text).

D. Electronic structure: Density of states

The pressure-induced liquid structural change is clearly related to the corresponding solid phases, which makes it likely that similar electronic effects are occurring. In previous work on crystalline Cs, the complex phases have been attributed to a change in electronic structure related first to an $s \rightarrow d$ electron transfer and then to a possible contribution from the 5*p* electronic orbital.[10,15]

At low pressure, solid and liquid Cs are well described as a free electron gas. As shown in Fig. 6 our calculated Fermi energy as a function of pressure is plotted against values deduced from experimental density[1] and the free electron value. It can be seen that the free electron picture holds up well to 4.3 GPa. Beyond this the Fermi energy lies below the value predicted by the free electron picture. In the free electron picture, this drop in Fermi energy can be interpreted as due to interaction with the Brillouin zone[13] and the opening of a pseudogap. In the localized orbital picture it is due to $s \rightarrow d$ transfer, which reduces the number of free *s*-type electrons. In both cases the number of free electrons at the Fermi energy drops, consistent with the observed dip in conductivity.[33,34] This appears as a weak feature in our liquid density of states (DOS) calculations [Figs. 7(b) and 7(g)].

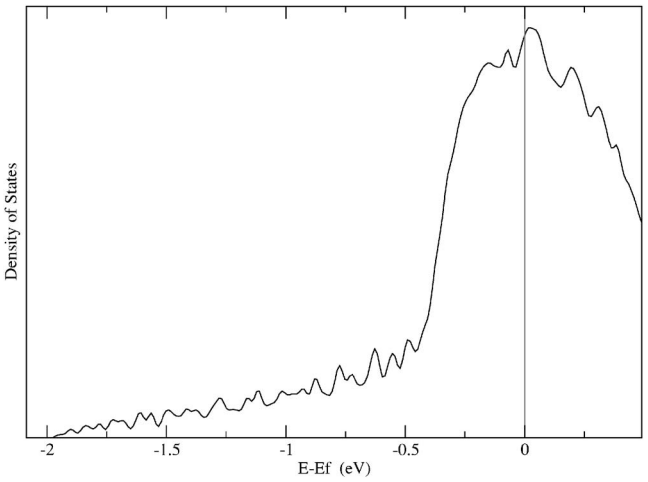

FIG. 8. Dense $(9\times9\times9)$ *k*-point sampling of DOS for 6*s*-only pseudopotential using a 64 atoms snapshot supercell taken from the 4.2 GPa calculation with the full pseudopotential. States are represented by Gaussians broadened by 0.02 eV.

Although the issue of $s \rightarrow d$ transfer has dominated previous discussion of the complex behavior of Cs, a recent study Tse[15] has shown that the valence electrons in Cs III lie primarily *between* atoms rather than on them, hence, the value of projection onto atom-centred orbitals is unclear. Notwithstanding that, the mathematical procedure is straightforward, and we have examined the angular character of the wave functions (Fig. 7, right panel). The density of states is calculated from states at the Γ point of the supercell. In view of the nonperiodic nature of a liquid, it appears to make no sense to examine other *k* points. However, the poor sampling offered by Γ-point-only sampling means that the free electrons are represented only at values of *k* commensurate with the supercell—hence, the distinct peaks at low energy corresponding to free electrons with pure *s* symmetry and wave vector commensurate with the supercell. For comparison, a calculation of the density of states with a less accurate pseudopotential with 5*p* electrons treated as core and a $9\times9\times9$ *k*-point mesh is presented in Fig. 8. This shows a smoother, broad distribution of *s*-states at low energy with the characteristic *d*-band peak starting some 0.4 eV below the Fermi energy. In considering our density of states calculation, it is thus more relevant to consider the character of the eigenstates than the overall shape of the DOS.

The liquid electronic structure results in the complex region are remarkably similar to the crystalline ones. The wave

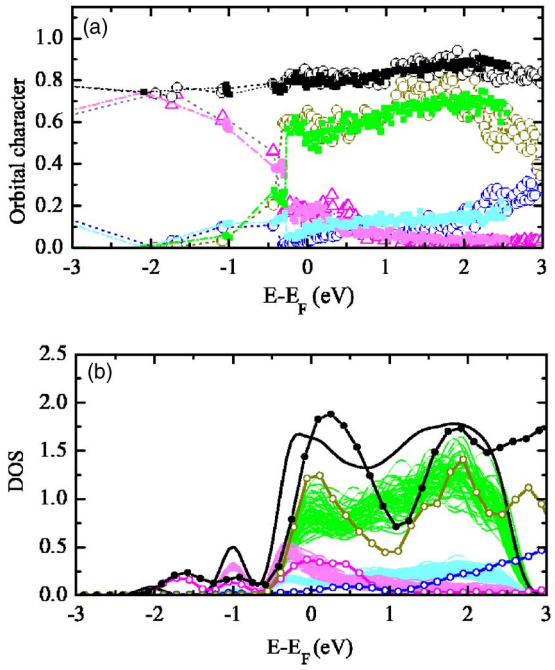

FIG. 9. (Color online) Equivalent figures to Fig. 7 showing (a) orbital character of each wave function and (b) projected DOS for Cs III and Cs liquid at the same pressure 4.2 GPa. All states are broadened by 0.2 eV to create the DOS. The colors represent: panel (a) Cs III solid: *s*-projection open up-triangles, *p*-projection blue open circles, *d*-projection dark yellow open circles, total DOS =black open circles; liquid states all have full squares: *s*-projection light magenta, *p*-projection light cyan, *d*-projection=green, total =thick black. Panel (b) has the same color/symbol scheme, except that the square symbols on the liquid lines are removed to show the variation between DOS curves taken from different snapshots of the liquid structure. The main feature to notice is that there are no "pure" angular momentum states—each wave function is strongly hybridized.

functions are delocalized across the sample, having significant projected weight on all atoms. Furthermore, there is a clear trend towards *s-d hybridization* rather than *transfer* with increasing pressure: i.e., each delocalized orbital is a mix of *s* and *d* character. This semantic difference has not been examined in previous work and our results are similar to our calculations on crystal structures, including the unstable simple phases. Thus the complex phases do not, of themselves, induce *s-d* transfer. The *d*-like character of the electrons depends strongly on density regardless of the crystal (or liquid) structure (Fig. 9) which strongly implies that the electronic structure drives the crystal structure, rather than vice-versa. This helps to explain the lack of distinct features in the liquid angular distribution function.

IV. CONCLUSIONS

We have shown that the properties of high pressure cesium crystal and liquid are reproduced by plane-wave DFT calculation in good agreement with experiment. The enthalpy of the various crystal structures I–IV is shown to be very similar in the transition region, with entropic effects probably playing a defining role in stabilizing Cs III and lowering the melting point.

The anomalous change in liquid near-neighbor distance is correctly reproduced. The electronic structure of both liquid and all four crystal structures shows sharply increasing *d* character via $s-d$ hybridization with pressure around 4 GPa. Ionic structure has a minimal effect. Thus, we conclude that the structural anomaly in the liquid phase has the same electronic effect as causes the stabilization of Cs III, namely the opening of a small pseudogap due to ion-electron interactions between the Brilloun zone boundary and the Fermi energy. This is manifest as a dip in the electronic density of states at the Fermi energy, leading to low energy phonons, decreased conductivity and Bragg peaks at $2k_F$ as we have noted previously for simple metals.[23,35,36] Since $2k_F$ is not compatible with Bragg peaks of simple structures, this effect is also associated with incommensurate phases[37] and lowered melting point.

In the liquid, it is still possible to lower the energy of the electrons by scattering them if the ions line up with particular periodicity (i.e., $2k_F$, in any direction). The lack of long range order means no Bragg Peaks and no Brillouin zone, but the preferential scattering should still occur, and we should see a peak in $S(q)$ at $q=2k_F$. In fact, this manifests in the experimental data as a shoulder on the main peak.[1]

ACKNOWLEDGMENTS

The authors thank the Edinburgh Parallel Computing Centre (EPCC) of The University of Edinburgh for the CPU time allocation, and M. I. McMahon and R. D'Agosta for helpful discussions.

[1] S. Falconi, L. F. Lundegaard, C. Hejny, and M. I. McMahon, Phys. Rev. Lett. **94**, 125507 (2005).
[2] J. P. Hansen and I. R. McDonald, in *Theory of Simple Liquids* (Academic Press, London, 1990).
[3] N. W. Ashcroft and J. Lekner, Phys. Rev. **145**, 83 (1966).
[4] J. Chihara and G. Kahl, Phys. Rev. B **58**, 5314 (1998).
[5] T. Hattori, K. Tsuji, N. Taga, Y. Takasugi, and T. Mori., Phys. Rev. B **68**, 224106 (2003), and references therein; T. Hattori, N. Taga, Y. Takasugi, T. Mori J., and K. Tsuji, J. Phys.: Condens. Matter **14**, 10517 (2002); K. Tsuji, T. Hattori, T. Mori, T. Kinoshita, T Narushima, and N. Funamori, *ibid.* **16**, S989 (2004).
[6] M. I. McMahon, R. J. Nelmes, and S. Rekhi, Phys. Rev. Lett. **87**, 255502 (2001).
[7] K. Takemura, S. Minomura, and O. Shimomura, Phys. Rev. Lett. **49**, 1772 (1982); K. Takemura and K. Syassen, Phys. Rev. B **32**, 2213 (1985).
[8] N. E. Christensen, D. J. Boers, J. L. van Velsen, and D. L. Novikov J. Phys.: Condens. Matter **12**, 3293 (2000); Phys. Rev. B

61, R3764 (2000).
[9] H. T. Hall, L. Merrill, and J. D. Barnett, Science **146**, 1297 (1964).
[10] M. Ross and A. K. McMahan, Phys. Rev. B **26**, 4088 (1982).
[11] A. K. McMahan, Phys. Rev. B **29**, R5982 (1984).
[12] G. J. Ackland and S. K. Reed, Phys. Rev. B **67**, 174108 (2003).
[13] G. J. Ackland, *Proceedings of Solid-Solid Phase Transformations in Inorganic Materials*, Phoenix, May 2005. TMS (2005); *Solid-Solid Phase Transformations in Inorganic Materials 2005*, vol. 2 TMS, edited JM Howe, DE Laughlin, JK Lee, U Dahmen, and WA Soffa (Warrendale, PA, 2005); cond-mat/0509454 (unpublished).
[14] J. M. Osorio-Guillen, R. Ahuja, and B. Johansson, ChemPhysChem **5**, 1411 (2004) present a detailed calculation of Cs II–V. Their claim to find a stable Cs III phase is erroneous, since at the claimed volume a mixture of Cs II and Cs IV clearly has lower energy (see their Fig. 3). Despite the difference in interpretation, their actual calculation results of relative enthalpies are essentially identical to ours.
[15] J. S. Tse, Z. Kristallogr. **220**, 521 (2005).
[16] K. Tsuji, K. Yaoita, M. Imai, T. Mitamura, T. Kikegawa, O. Shimomura, and H. Endo, J. Non-Cryst. Solids **117/118**, 72 (1990); Y. Katayama and K. Tsuji, J. Phys.: Condens. Matter **15**, 6085 (2003).
[17] A. Jayaraman, R. C. Newton, and J. M. McDonough, Phys. Rev. **159**, 527 (1967).
[18] M. M. Abd-Elmeguid, H. Pattyn, and S. Bukshpan, Phys. Rev. Lett. **72**, 502 (1994).
[19] Y. Kong and O. Jepsen, J. Phys.: Condens. Matter **12**, 8973 (2000).
[20] S. P. Chen, J. S. Tse, D. D. Klug, L. Zhiqiang, U. Kentaro, and L. G. Wang, Phys. Rev. B **62**, 3624 (2000).
[21] I. Loa, K. Kunc, K. Syassen, M. Krisch, A. Mermet, and M. Hanfland, High Press. Res. **23**, 1 (2003).
[22] V. Heine, Solid State Phys. **24**, 1 (1970).
[23] G. J. Ackland and I. R. MacLeod, New J. Phys. **16**, S2629 (2004).
[24] G. Kresse, cms.mpi.univie.ac.at/vasp/
[25] J. P. Perdew, J. A. Chevary, S. H. Vosko, K. A. Jackson, M. R. Pederson, D. J. Singh, and C. Fiolhais, Phys. Rev. B **46**, 6671 (1992).
[26] H. Akbarzadeh, S. J. Clark, and G. J. Ackland, J. Phys.: Condens. Matter **5**, 8065 (1993).
[27] M. Parrinello and A. Rahman, J. Appl. Phys. **52**, 7182 (1981).
[28] S. Nosé, J. Chem. Phys. **81**, 511 (1984).
[29] The 64 atom cells use a simple cubic initial structure at ambient, then on pressure increase the final cell is reused. The 264 cell used starting coordinates from a fcc+interstitial cell replicated eight times. M. I. Mendelev, D. J. Srolovitz, G. J. Ackland, S. Han, and J. R. Morris (unpublished).
[30] G. J. Ackland and H. Fox, J. Phys.: Condens. Matter **17**, 1859 (2005).
[31] K. Syassen, in *Proc. Int. School of Physics "Enrico Fermi," Course 147*, Varenna, Italy, 2001, edited by R. J. Hemley (IOS, Amsterdam, 2002).
[32] G. Burns, *Solid State Physics* (Academic Press, London, 1985).
[33] R. A. Stager and H. G. Drickamer, Phys. Rev. Lett. **12**, 19 (1964).
[34] G. C. Kennedy, A. Jayaraman, and R. C. Newton, Phys. Rev. **126**, 1363 (1962); A. Jayaraman, R. C. Newton, and J. M. McDonough, *ibid.* **159**, 527 (1967).
[35] E. G. Maksimov, M. V. Magnitskaya, and V. E. Fortov, Phys. Usp. **48**, 761 (2005).
[36] R. Boehler and C. S. Zha, Physica B **139**, 233 (1986).
[37] S. K. Reed and G. J. Ackland, Phys. Rev. Lett. **84**, 5580 (2000).